Muon Capture in Gaseous Hydrogen

A. ALBERIGI QUARANTA,* A. BERTIN, G. MATONE,† AND F. PALMONARI
Instituto di Fisica dell' Università di Bologna, and Instituto Nazionale di Fisica Nucleare, Sezione di Bologna, Italy

AND

G. TORELLI
Instituto di Fisica dell' Università di Pisa, and Instituto Nazionale di Fisica Nucleare, Sezione di Pisa, Italy

AND

P. DALPIAZ, A. PLACCI, AND E. ZAVATTINI
CERN, Geneva, Switzerland

(Received 22 August 1968)

An experiment to measure the muon nuclear capture rate in ultrapure gaseous hydrogen (8 atm, 293°K) has been performed using a special target in which a system of gas proportional counters, working with the pure hydrogen of the target itself, were operating. Neutrons from the capture reactions were detected using a scintillation-counter technique, and the γ-ray background was eliminated by pulse-shape discrimination. The working conditions ensured that the captures were taking place in μp atomic systems in a singlet total-spin state. The experimental result is $\Lambda_{\text{expt}}=651\pm57$ sec^{-1}, which has to be compared with the theoretical rate $\Lambda_{s,\text{ theor}}=626\pm26$ sec^{-1}. From the experimental capture rate, and within the framework of the currently accepted theory, we have obtained for the induced pseudoscalar coupling constant $g_P=(-7.3\pm3.7)g_V$. The results of the present experiment are analyzed, together with results obtained from stopping negative muons in liquid hydrogen.

1. INTRODUCTION

A. Purpose of Experiment

We describe here a measurement of the nuclear capture rate of a negative muon by a free proton according to the reaction

$$\mu^-+p\rightarrow n+\nu_\mu, \qquad (1)$$

when the muon-proton system is in a singlet state.

The experimental data so far available regarding process (1), observed by Hildebrand[1] for the first time in a bubble-chamber experiment, were all obtained by stopping negative muons in liquid hydrogen.[1–4] Quite a lot of experimental[5,6] and theoretical work[7–9] was done to clarify the different processes in which a negative muon is involved after stopping in liquid hydrogen, and it is currently believed that in this case reaction (1) occurs to the greatest extent while the muon is bound in a $p\mu p$ muonic molecule. It has therefore been possible to give accurate specifications of the initial muon-proton total-spin state, and to compare the observed rates $\Lambda_{M,\text{expt}}$ for reaction (1) with the corresponding theoretical predictions $\Lambda_{M,\text{theor}}$[10–13]. The values obtained by different experimental teams for the muon nuclear capture rate in liquid hydrogen are listed in Table I with the corresponding theoretical predictions as calculated by Kabir.[13]

We have performed the measurement of the rate of process (1) by stopping negative muons in deuterium-free highly purified gaseous hydrogen at 8 atm pressure and 293°K. The experiment was carried out in view of the following possibilities:

(i) to obtain a measurement of the rate of the elementary process (1) without μ-molecular complications, in order to check more directly the present agreement between theory and experiment (see Table I);

* Present address: Instituto di Fisica dell' Universitá di Modena, Modena, Italy.

† Present address: Laboratori Nazionali di Frascati, Italy.

[1] R. Hildebrand, Phys. Rev. Letters **8**, 34 (1962); R. Hildebrand and J. H. Doede, in *Proceedings of the International Conference on High-Energy Physics, Geneva, 1962*, edited by J. Prentki (CERN Scientific Information Service, Geneva, 1962), p. 418; J. H. Doede and R. Hildebrand, cited by C. Rubbia in Proceedings International Conference on Fundamental Aspects of Weak Interactions, Brookhaven, 1963, p. 277 (unpublished).

[2] E. J. Bleser, L. M. Lederman, J. L. Rosen, J. E. Rothberg, and E. Zavattini, Phys. Rev. Letters **8**, 288 (1962).

[3] E. Bertolini, A. Citron, G. Gialanella, S. Focardi, A. Mukhin, C. Rubbia, and F. Saporetti, in *Proceeding of the International Conference on High-Energy Physics, Geneva, 1962*, edited by J. Prentki (CERN Scientific Information Service, Geneva, 1962), p. 421. S. Focardi, G. Gialanella, C. Rubbia, and F. Saporetti, cited by C. Rubbia, in Proceedings of the International Conference on Fundamental Aspects of Weak Interactions, Brookhaven, 1963, p. 278 (unpublished). The partial Bologna result is $\Lambda_{M,\text{expt}}=427\pm83$ sec^{-1} [S. Focardi (private communication)].

[4] J. E. Rothberg, E. W. Anderson, E. J. Bleser, L. M. Lederman, S. L. Meyer, J. L. Rosen, and I. T. Wang, Phys. Rev. **132**, 2664 (1963).

[5] G. Conforto, C. Rubbia, E. Zavattini, and S. Focardi, Nuovo Cimento **33**, 1001 (1964).

[6] E. J. Bleser, E. W. Anderson, L. M. Lederman, S. L. Meyer, J. L. Rosen, J. E. Rothberg, and I. T. Wang, Phys. Rev. **132**, 2679 (1963).

[7] S. Cohen, D. L. Judd, and R. J. Riddell, Phys. Rev. **119**, 397 (1960).

[8] V. B. Belyaev, S. S. Gershtein, N. B. Zakharev, and S. P. Lemnev, Zh. Eksperim. i Teor. Fiz. **37**, 1652 (1959) [English transl.: Soviet Phys.—JETP **10**, 1171 (1960)].

[9] Y. B. Zel'dovich and S. S. Gershtein, Usp. Fiz. Nauk **71**, 581 (1961) [English transl.: Soviet Phys.—Usp. **3**, 593 (1961)].

[10] H. Primakoff, Rev. Mod. Phys. **31**, 802 (1959); J. Bernstein, T. D. Lee, C. N. Yang, and H. Primakoff, Phys. Rev. **111**, 313 (1958).

[11] S. Weinberg, Phys. Rev. Letters **4**, 585 (1960).

[12] A. Halpern, Phys. Rev. **135**, A34 (1964).

[13] P. K. Kabir, Z. Physik **191**, 447 (1966).

TABLE I. Experimental results and corresponding theoretical predictions on the rate of the reaction $\mu^-+p\rightarrow n+\nu_\mu$.

Authors	Type of H_2 target	Technique	$\Lambda_{M,\text{expt}}$ (sec^{-1})	Λ_{expt} (sec^{-1})	$\Lambda_{M,\text{theor}}$ (sec^{-1})	$\Lambda_{s,\text{theor}}$[a] (sec^{-1})	$\Lambda_{t,\text{theor}}$[a] (sec^{-1})
Chicago[b]	liquid	bubble chamber	428±85		494±21[c]		
Columbia[d]	liquid	counters	515±85		477±20		
CERN-Bologna[e]	liquid	bubble chamber	450±50		494±21[c]		
Columbia[f]	liquid	counters	464±42		477±20		
CERN-Bologna (present expt.)	gaseous	counters		651±57		626±26	12

[a] Equations (16)–(18) give the values for $g_P g_V$, g_A/g_V, and g_V used by Kabir to derive these rates.
[b] See Ref. 1.
[c] This number is larger than 477 sec^{-1}, because in the bubble-chamber experiments muons could be captured also in μp muonic atoms before they formed $p\mu p$ muonic molecules; the correction has been obtained using the $\Lambda_{s,\text{theor}}$ given in this table and the λ_{pp} μ-molecular formation rate given by Conforto *et al.* (Ref. 5) referring to a liquid-hydrogen density of 3.5×10^{22} atoms/cm^3. It has been assumed that the μp systems will always be in a singlet state.
[d] See Ref. 2.
[e] See Ref. 3.
[f] See Ref. 4.

(ii) to get a value for the nuclear capture rate in a different total spin combination for the muon-proton system; the knowledge of these quantities in two different spin states will then supply a direct experimental check of the universality of the $V-A$ weak-interaction coupling theory;[10–14] and

(iii) to obtain another independent measurement which, combined with the existing ones, will lead to a more precise value of the induced pseudoscalar coupling constant.

Preliminary results of this measurement have already been published,[15] and the purpose of this paper is to describe the experiment in detail, and to give the final results.

B. μp Muonic Atom

A negative muon slowing down in isotopically pure hydrogen forms at first an excited μp muonic atom, which promptly decays to its lowest orbital level. To ensure that a muon spends most of its lifetime in a μp system before decaying, the density ρ of the hydrogen within which the muonic atom is formed must satisfy the limitation

$$\rho\ll\frac{\lambda_0}{\lambda_{pp}}\rho_l=7.5\times10^{21}\ \text{atoms/cm}^3, \qquad (2)$$

where λ_0 is the decay rate of the free muon ($\lambda_0=4.548\times10^5\ \text{sec}^{-1}$), and λ_{pp} is the μ-molecular formation rate at the density of liquid hydrogen ρ_l as given in Ref. 5. In our experimental conditions (8 atm, 293°K) we have

$$\rho=4\times10^{20}\ \text{atoms/cm}^3, \qquad (3)$$

so that 95% of the incoming muons decay while they are still bound in μp muonic atoms; the remaining ones form $p\mu p$ muonic molecules.

The μp system can exist in two hyperfine structure states, i.e., the $F=0$ singlet state and the $F=1$ triplet state, F being the total spin of the muonic atom. The energy difference between these two states is given by[16]

$$\Delta E=(16/3)\pi\beta_\mu\beta_n g|\psi(0)|^2=0.18\ \text{eV}, \qquad (4)$$

where β_μ is the muonic and β_n is the nuclear Bohr magneton, and g is the gyromagnetic ratio of the proton.

The theoretically predicted nuclear capture rates in the singlet ($\Lambda_{s,\text{theor}}$) and in the triplet states ($\Lambda_{t,\text{theor}}$) are also shown in Table I. In order to compare the experimental results with such predictions, it is then necessary to know which fraction of the μp muonic atoms is in a singlet state at any given time, i.e., to know how the total spin of the muonic atom evolves in time as a result of the collisions that such a system undergoes with the surrounding hydrogen molecules.

The life story of the μp systems after their formation has been clarified by the analysis of Zel'dovich and Gershtein;[9,17] in the following, we give a brief summary of their main conclusions, some of which have been verified experimentally.[18]

The μp muonic atoms are initially formed in a statistical mixture of triplet and singlet states, and their average kinetic energy E_0 is between 0.5 and 1 eV,[18,19] i.e., rather higher than ΔE. It has been shown by Gershtein that the scattering cross section $\sigma_{1,0}$ of these relatively energetic muonic atoms against the hydrogen molecules is very high, so that the muonic atoms are rapidly slowed down. He has also shown that when the kinetic energy of a μp system is less than 0.18 eV, the cross section $\sigma_{1\to0}$ for scattering against a hydrogen molecule with the μp muonic atoms changing from the

[14] R. P. Feynman and M. Gell-Mann, Phys. Rev. **109**, 193 (1958); E. C. G. Sudarshan and R. E. Marshak, *ibid.* **109**, 1860 (1958); Ya.B. Zel'dovich and S. S. Gershtein, Zh. Eksperim. i Teor. Fiz. **35**, 821 (1958) [English transl.: Soviet Phys.—JETP **8**, 570 (1959)].
[15] A. Alberigi Quaranta, A. Bertin, G. Matone, F. Palmonari, A. Placci, P. Dalpiaz, G. Torelli, and E. Zavattini, Phys. Letters **25B**, 429 (1967).
[16] E. Fermi, Z. Physik **60**, 320 (1930).
[17] S. S. Gershtein, Zh. Eksperim. i Teor. Fiz. **34**, 463 (1968); **36**, 1309 (1959) [English transls.: Soviet Phys.—JETP **7**, 1171 (1958); **9**, 927 (1959)].
[18] A. Alberigi Quaranta, A. Bertin, G. Matone, F. Palmonari, A. Placci, P. Dalpiaz, G. Torelli, and E. Zavattini, Nuovo Cimento **47B**, 72 (1967).
[19] V. P. Dzhelepov, P. F. Ermolov, V. I. Moskalev, V. V. Filchenkov, and M. Friml, Zh. Eksperim. i Teor. Fiz. **47**, 1923 (1964) [English transl.: Soviet Phys.—JETP **20**, 841 (1965)].

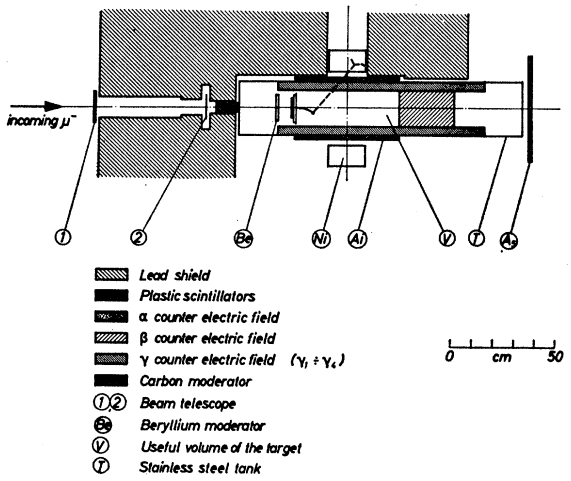

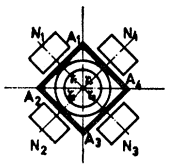

FIG. 1. Simplified scheme of the experimental arrangement used to measure the nuclear capture rate of negative muons by free protons in a gaseous target.

triplet to the singlet states is also extremely high. The singlet-to-triplet transition at these energies is in general not possible.[20]

It can then be shown that at the hydrogen density chosen in the present experiment, all the μp muonic atoms pass into the singlet state within a time interval which is certainly shorter than 100 nsec after their formation, and that after this time their average kinetic energy is less than 0.18 eV. From this moment on, the calculations show that the elastic scattering cross section σ_0 of μp muonic atoms against the hydrogen molecules is much smaller than $\sigma_{1,0}$ and $\sigma_{1\to 0}$.

In Table II the predicted values for $\sigma_{1,0}$, $\sigma_{1\to 0}$, and σ_0 are listed as calculated by Zel'dovich and Gershtein,[9] and by Cohen, Judd, and Riddell.[7] The last row shows the corresponding experimental results obtained by Alberigi Quaranta *et al.*[18]

C. Detection of Nuclear Capture Events

The experimental value Λ_{expt} for the nuclear capture rate of negative muons by protons is defined in our case by

$$\Lambda_{\text{expt}}=\lambda_0\frac{N}{ME}l\left(1+\frac{Nl}{ME}\right), \tag{5}$$

where N is the number of neutrons due to process (1) detected by the apparatus when M negative muons are stopped in hydrogen, E is the over-all efficiency of the apparatus for detecting the capture neutrons, and l is a correction factor which takes account of the small amount of $p\mu p$ μ-molecular formation. From the $\Lambda_{M,\text{theor}}$ value calculated by Kabir (see Table I) one gets, in our conditions, $l=1.01$.

TABLE II. Theoretical and experimental results on the scattering cross sections for the process $\mu p+p\to\mu p+p$.

Authors	$\sigma_0(10^{-21}$ cm$^2)$	$\sigma_{1\to 0}(10^{-19}$ cm$^2)$	$\sigma_{1,0}(10^{-19}$ cm$^2)$
Zel'dovich and Gershtein[a]	1.2	7.8	7.9
Cohen *et al.*[b]	8.2	3.9	4.0
Alberigi Quaranta *et al.*[c]	7.6±0.7	8.7±0.7[d] 4.0±0.5[d]	8.8±0.7[d] 4.1±0.5[d]

[a] See Ref. 9.
[b] See Ref. 7.
[c] See Ref. 18.
[d] The measured value for σ_0 leads to two possible values for $\sigma_{1,0}$ and $\sigma_{1\to 0}$.

[20] At $T=293°$K, $\frac{3}{2}kT=0.038$ eV.

In the present experiment the neutrons were detected by liquid scintillation proton-recoil counters, in analogy with the previous counter experiments;[2,4] a pulse-shape discrimination technique along the lines developed by Brooks[21] was used to eliminate the γ-ray background. The quantity M was determined by looking at the electrons due to muons decaying from the μp systems formed in the gaseous hydrogen. The electrons were detected by systems of counters (electron telescopes) which also included the liquid scintillation counters used as neutron detectors. Equation (5) can then be written

$$\Lambda_{\text{expt}}=\lambda_0 l\frac{NE_e}{N_eE}\left(1+\frac{NE_el}{N_eE}\right), \tag{6}$$

where N_e is the number of electrons detected by the electron telescopes corresponding to M muons stopping in hydrogen, and E_e is the over-all efficiency of the apparatus for counting electrons. The quantities E and E_e are to be calculated.

The experimental arrangement was designed bearing in mind that besides eliminating the γ-ray background, it was also essential to eliminate the following background neutrons:

(i) neutrons due to the nuclear capture of muons by extraneous elements, contained as impurities in the gaseous hydrogen;
(ii) neutrons due to nuclear capture of muons stopping directly in elements other than hydrogen, which were part of the target itself;

[21] F. D. Brooks, Nucl. Instr. Methods 4, 151 (1959); F. D. Brooks, Prog. Nucl. Phys. 5, 252 (1956).

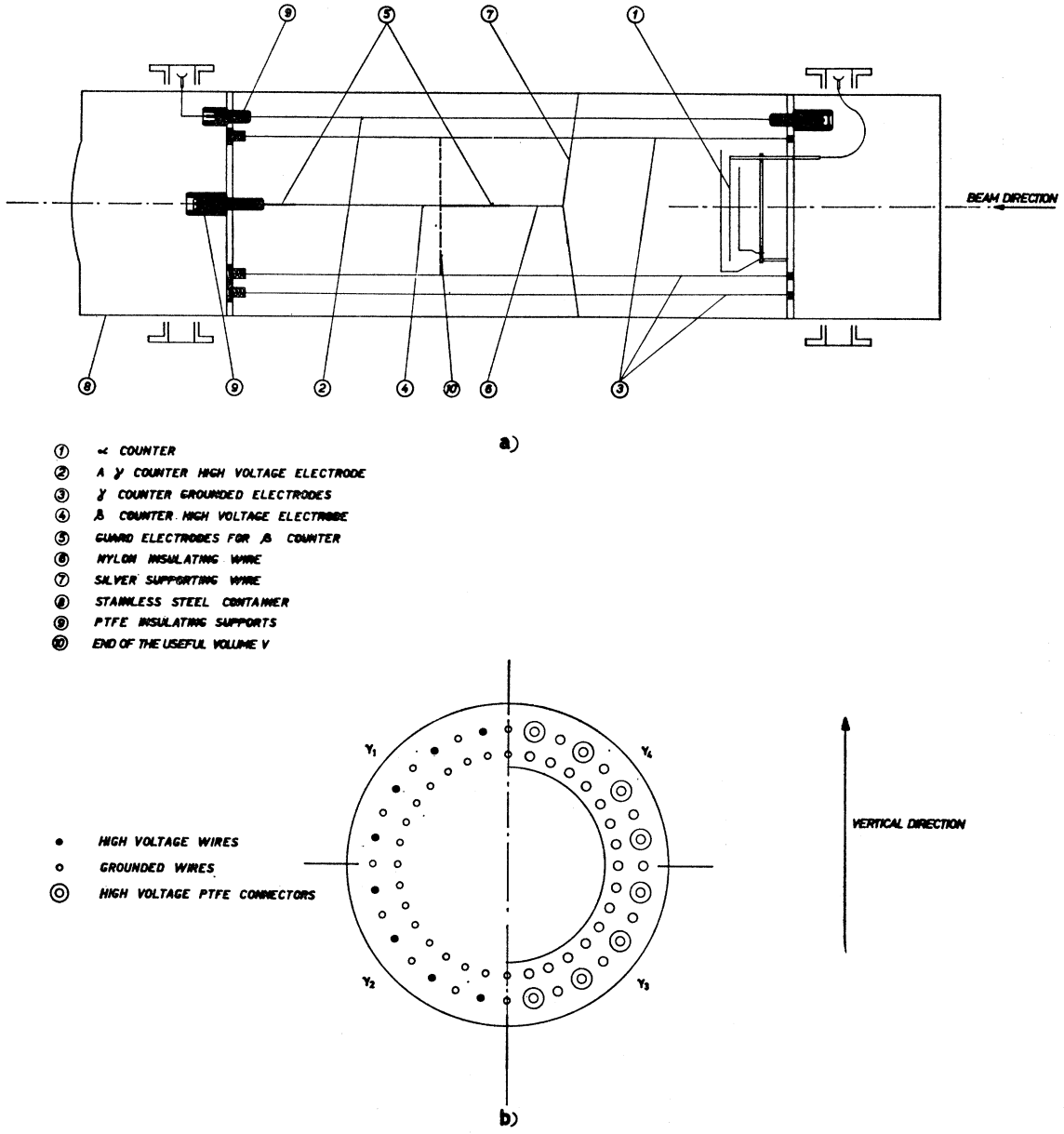

FIG. 2. Schematic drawing of the special protium target: (a) side view of the container and of the complete structure of wire porportional counters working in the gaseous protium; (b) geometry of the wires of counter γ and of the four γ_i sections.

(iii) neutrons coming from $N(\gamma,n)N'$ reactions on the materials surrounding the apparatus. Particularly dangerous were those neutrons generated by the bremsstrahlung γ-rays from the decay electrons of muons stopped in hydrogen; the time distribution of these neutrons is, in fact, equal to the time distribution of the neutrons coming from process (1);

(iv) accidental neutrons;

(v) neutrons due to the nuclear capture of muons transferred to the atoms of the wall of the container by the diffusing neutral μp muonic atoms. Using the values reported in Table II, it has been shown by Alberigi Quaranta *et al.*[18] that the total number of muons transferring to the walls can be as high as 2% of the μp muonic atoms present in the gaseous hydrogen. These neutrons, too, are specially misleading, since their time distribution is quite similar to that of neutrons coming from reaction (1).

The background neutrons due to (i) were eliminated using deuterium-free hydrogen (protium), and by filtering it with a palladium purifier before entering the target. The background neutrons due to the other

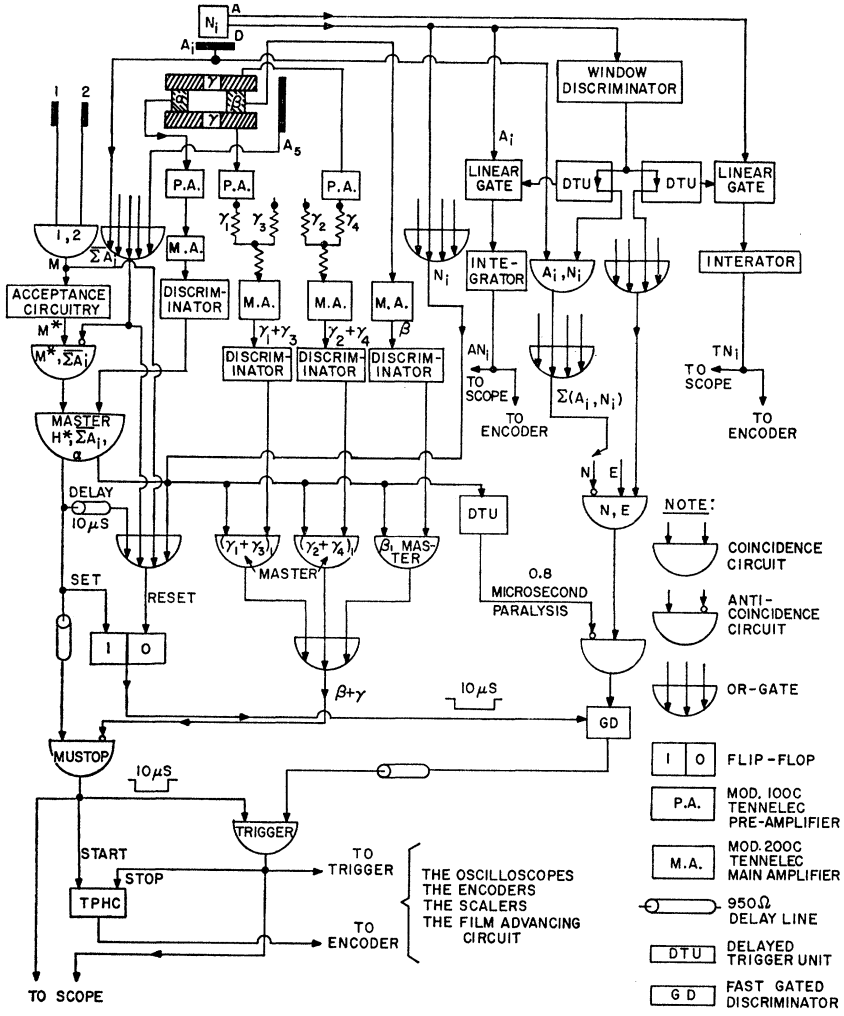

FIG. 3. Simplified block diagram of the electronics.

sources [(ii) to (v)] were eliminated or were reduced to an acceptable level, mainly by introducing into the target, all around the internal surface of the cylindrical container, a series of wire proportional counters working with the pure hydrogen of the target itself as a filling gas; these counters operated with an anticoincidence function for charged particles in the trigger logic (see Sec. 2).

Moreover, the neutrons due to the effect mentioned in (ii) were further reduced by accepting only those neutrons that were delayed by more than 0.8 μsec with respect to the incoming muon. The target and all the materials surrounding it were made up exclusively of elements (Fe, Pb[22]) with high atomic number [the only exceptions were the PTFE H.V. insulators which, however, were shielded from the incoming μ^- by regions of the anticoincidence proportional counters (see Fig. 2)].

A simplified view of the experimental setup used for the measurements is shown in Fig. 1.

From the foregoing, it is quite clear that the capture processes observed in the present experiment took place while the μp muonic atoms were all in a singlet state; in other words, our Λ_{expt} can be directly compared to the $\Lambda_{s,\text{theor}}$ of Table I. A calculation of the population η of the triplet states of the μp muonic atoms after 0.9 μsec, even taking into account the existence of ortho- and para-excited states (at 293°K) for the hydrogen molecules, shows that η is much less than 1%.

2. EXPERIMENT

A. The Target

The cylindrical vessel containing the protium was of a special design and, as mentioned, contained a system of three wire proportional counters which worked by using the protium itself as a filling gas. This device has been described in detail elsewhere;[23] here we will

[22] The lifetimes of negative muons stopped in iron and lead are 0.2 and 0.08 μsec, respectively (see Ref. 37).

[23] A. Alberigi Quaranta, A. Bertin, G. Matone, F. Palmonari, A. Placci, P. Dalpiaz, and E. Zavattini, Nucl. Instr. Methods **55**, 273 (1967).

give a short summary of its structure and main characteristics.

The container was a stainless-steel cylinder, 260 mm in diam and 1352-mm long, closed by flanges at both ends. It was constructed with a reduced thickness both in the central part of the front flange (1-mm entrance window) and in that part of the side surface which had to face the neutron counters (2.5 mm); it had also to satisfy severe requirements of pressure and vacuum tightness (up to 25 atm and 10^{-7} Torr, respectively). Furthermore, the inside surface was made perfectly smooth so as to avoid electrostatic discharges due to the high electric fields involved in the operation of the above-mentioned proportional counters; the whole tank, electrolytically cleaned, was degassed for 15 days under vacuum before beginning the experiment.[24] Several side outputs were open on the walls of the target. Some of these were connected by pressure valves and vacuum-tight valves to the filling system, which included the evacuating-filling facilities, as well as vacuum and pressure control, and the safety devices. The remaining side outputs were used to supply the high voltage to the wire proportional counters and to collect their signals, the contacts being ensured by special high-voltage glass feedthroughs.

Three different wire proportional counters were placed inside the container and mounted on a frame which could freely move within the cylinder (see Fig. 2):

(a) A grid plane-structure counter (α counter) was placed in front of the entrance window, and was required to operate in relatively fast coincidence in order to define the incoming beam; its construction was such that its total time jitter was about 0.5 μsec. It was made of three grids: a 10-cm diam cathode; a 13-cm diam HV counting grid; and a 15-cm diam shielding cathode downstream from the beam. Each grid was made of a few parallel stainless-steel wires, with maximum diameter of 100 μ and spacing 6 mm apart.

(b) A peripheral counter (γ counter) was made up of a series of 16 quasicylindrical wire proportional counters, obtained by suitably grouping grounded wires around the high-voltage wires all along the internal side surface of the container; these stainless-steel wires also had a maximum diameter of 100 μ, and those of them that were used as high-voltage electrodes were fixed to the grounded structure of the container by hollow PTFE insulators. The γ counter operated producing anticoincidence signals for each charged particle arriving at a distance less than 4.4 cm from the side surface of the container.

(c) A cylindrical counter (β counter) was situated in the back of the container, and had the same anticoincidence functions as the γ counter, but with respect to the back wall of the tank. Counter β had a diameter of 172 mm and an active length of 260 mm.

[24] The container was supplied by SIAI-LERICI, Cormano, Milano, Italy.

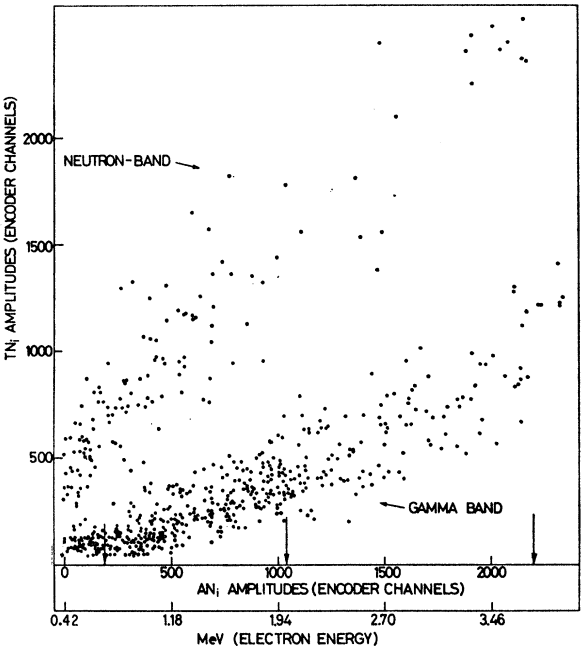

FIG. 4. A typical two-dimensional plot of the AN_i and TN_i encoder outputs. These points correspond to not yet selected events, detected by counter N_3 and recorded in correspondence with 65×10^7 accepted monitors. The arrows on the horizontal scale show the low-energy cut operated during the analysis (left arrow), the channel corresponding to 5.2 MeV (neutron energy), and the upper energy cut (right arrow).

An $\alpha\bar{\beta}\bar{\gamma}$ signal defined a muon stopping in the useful volume V of hydrogen which was delimited by the proportional counters, and which was therefore a region whose boundary was marked by only a few extremely thin wires. The volume thus defined was that of a cylinder 491 mm long with a diameter of 172 mm.

The signals of α, β, and γ counters were sent through short cables to TENNELEC 100C charge-sensitive preamplifiers, the outputs of which were sent through 10-m long cables to TENNELEC 200C amplifiers (see Fig. 3).

The three wire proportional counters worked under the conditions listed in Table III, where the differentiation and integration constants and the gain of their amplitudes are also given.

Counter γ (see Fig. 2) was divided into four sections (γ_1–γ_4), each of which was connected to one preamplifier, to divide up the considerable capacity of the whole

TABLE III. Working conditions of the wire proportional counters and of the corresponding amplifiers (gas pressure: 8 atm of pure hydrogen).

		Amplifier characteristics			
Counter	HV power supply (kV)	1st diff. const. (μsec)	2nd diff. const. (μsec)	Integr. const. (μsec)	Gain
α	15	3.2	0.8	3.2	64
β	19	1.6	1.6	1.6	1
γ	8.2	1.6	0.8	1.6	8

counter (about 300 pF). A linear mixing was carried out successively for the γ_1 and γ_3 signals, and separately for the γ_2 and γ_4 ones, before sending them to the amplifiers and to the rest of the electronic logic.

The dimensions of the wire proportional counters β and γ were chosen so that muons forming μp atoms in the volume V certainly decayed before the muonic atoms could diffuse up to the container walls. Counter β was actually overdimensioned lengthwise, because the tank was prepared in such a way that it could, in the future, be used with a larger number of neutron counters.

The target was filled with pure protium,[25] which was recycled every day through a palladium purifier[26] to ensure a high degree of purity.[27] It is worthwhile mentioning here that the behavior of the proportional counters (especially that of counter β, due to its large diameter) proved to be a rather sensitive tool for checking the air contamination of the purified protium. It was possible to verify that the gaseous protium remained pure to better than 1 ppm with respect to air over a period of one day.[23]

B. Neutron Counters

Four proton-recoil liquid scintillators were used as neutron detectors. They were made of NE-213 liquid contained in cylindrical glass cells, 4-in. long and 7 in. in diam.[28] Each cell was viewed directly by a 54 AVP photomultiplier. The surface not used for light collection was covered by a reflective coating of compressed magnesium oxide. The neutron counters (N_i) were disposed symmetrically around the target, and placed in cylindrical cavities made in the lead shielding blocks (see Fig. 1). A layer of paraffin covered the whole apparatus. The materials present between the sensitive volume of each N_i counter and the gaseous hydrogen were iron (2.8 mm), plastic scintillator (15 mm), scotch tape (1 mm), glass (3 mm,) and magnesium oxide (2 mm).

The pulse-shape discrimination for resolving neutrons from γ rays was obtained as follows (see Fig. 3). The pulses coming from the anode (A) and from the last dynode (D) of each N_i photomultiplier were sent to two integrators via very stable linear gates.[29] The linear gates were driven by properly delayed pulses, so that one integrator produced a signal (AN_i) proportional to the area of that part of the scintillation pulse contained between its beginning (t_0) and about 50 nsec after (t_1), whereas the other one integrated that part of the pulse contained between 60 nsec (t_2) and 200 nsec (t_3) after t_0 (TN_i signal).

Both the AN_i and the TN_i signals were sent to two 2500-channel analog-to-digital converters (encoders). The maximum channel of the encoder which received the AN_i signals corresponded to an energy loss of about 4 MeV (electron energies). The AN_i signals were also sent to an oscilloscope track.

Figure 4 shows how pulses corresponding to neutrons and γ rays distributed themselves on an (AN_i,TN_i) plane, occupying two well-defined regions (γ and neutron band). The optimization of these figures was achieved for each counter, using a Po-Be source and varying the different delays involved (t_0–t_3). Sources of neutrons and γ rays were periodically used to check the stability of the positions of the neutron and γ bands.

Measurements with the mentioned sources have shown that near the amplitude corresponding to 0.72 MeV (electron energy) in the worst case about 2% of the detected γ rays were giving their representative point within the neutron band; of course at higher energy such "contamination" becomes negligible.

The N_i photomultipliers were set to work in rigorously linear conditions for pulses corresponding to energies up to 6 MeV (electron energies). The energy scale and the energy resolution for the AN_i pulses were measured periodically by means of radioactive sources supplying γ rays of suitable energies (^{60}Co, ^{22}Na, and ^{24}Na). The spectra obtained from these sources were then analysed by a Monte Carlo calculation, which supplied both the electron energy scale and the energy resolution. In the working conditions, the energy resolution of our N_i counters was about 16% for the second peak of the ^{24}Na source.

C. Fast Counters

Two fast plastic scintillators (counters 1 and 2, see Fig. 1) were monitoring the incoming beam.[30] Four other plastics A_i were disposed around the target as the four sides of a square box, between the target and the corresponding neutron counter N_i.[31] Each A_i was used either in fast coincidence with the corresponding N_i counter (electron selection) or in fast anticoincidence with it (neutral selection). Another plastic scintillator A_5 was put after the back flange of the hydrogen target, to be used in fast anticoincidence with the counters defining the stopping beam.

D. Electronics

A simplified block diagram of the electronics used in the experiment is given in Fig. 3. The fast coincidence of counters 1 and 2 defined the incoming particles (monitor coincidence). The output pulses of the monitor

[25] The protium contained less than 3 ppm of deuterium; it was supplied by Air Liquide, Paris, France.
[26] Supplied by Engelhard Industries, Newark, N. J.
[27] J. R. Young, Rev. Sci. Instr. 34, 891 (1963).
[28] The glass cells filled with the NE-213 liquid were especially made by Nuclear Enterprises Ltd., Sighthill, Edinburgh, Scotland. The neutron counters used in the present experiment are extensively described in a forth coming paper [A. Bertin, A. Vitale, and A. Placci, Nucl. Instr. Methods (to be published)].
[29] B. Smith, Nucl. Instr. Methods 55, 138 (1967).
[30] The dimensions of counters 1 and 2 were 15×15×1 cm and 15×10×0.2 cm, respectively.
[31] All the A_i plastic scintillators were 1.5 cm thick.

coincidence were sent through a proper circuitry in order to charge up a capacitor C which discharged with a time constant of ~ 2.2 μsec. A monitor pulse was accepted (accepted monitor M^*) and sent to the following circuits only when the residual voltage on the condenser C was lower than $V_0 = e^{-4}Q/C$, where Q is the charge stored in C by a single monitor pulse. This was done to eliminate accidental counts due to those negative muons which previously entered the apparatus.

The particles entering the useful volume V of the target were selected by the fast coincidence of a $(M^*, \sim\sum A_i)$ signal (where $\sim$ means "not") with the pulse coming from the properly biased counter α (master coincidence). This coincidence was sufficiently fast, since, as we have already mentioned, the time fluctuations of the α-counter pulses were confined within 500 nsec.

The pulses coming from the proportional counters β and γ_i, properly mixed and discriminated, were put in slow anticoincidence with the master signal to define a particle stopping in V["mustop" signal $= (M^*, \sim\sum A_i, \alpha, \bar{\beta}, \bar{\gamma})$].

Since the time fluctuations of the signals coming from counters β and γ_i were quite significant (of the order of 10 μsec), the pulses coming from them were set in coincidence with the master signals before being sent to the mustop circuit. The time of the mustop signal was then correlated with the monitor time.

The electronics connected with the pulse-shape discrimination for neutrons and γ rays has already been described; each A_i counter always coincided with the corresponding N_i in a fast coincidence circuit, the two counters thus constituting an electron telescope (A_i, N_i). The electronics connected to the A_i and N_i detectors could operate with the rest of the logic in two different selective ways

(i) Neutral selection. In this case the pulses coming from the N_i neutron counters were properly discriminated in amplitude by a fast window discriminator [lower threshold (LT) = 0.3 MeV; upper threshold (UT) = 6 MeV, electron energies]. The output of this circuit anticoincided successively with the signals coming from the (A_i, N_i) electron telescope in the fast coincidence-anticoincidence circuit (N, E).

(ii) Electron selection. In this case the UT of the window discriminator was removed, and the (A_i, N_i) electron telescopes were put in fast coincidence with the N_i counters in the (N, E) circuit. The circuitry was arranged in such a way that it worked with only one electron telescope at a time.

The output pulses of the (N, E) circuit were accepted only after a fixed delay of 0.8 μsec after the monitor signal in both the neutral and the electron selection. They were then sent to a slow coincidence with the mustop signal (trigger coincidence) through a gated discriminator (GD). The gate to GD was opened by the master signal, and either closed automatically after 10 μsec, or before this time due to a second monitor pulse, or immediately after the passage of the N_i pulse itself. The gate to the GD circuit was as long as 10 μsec in order to accept also delayed accidentals.

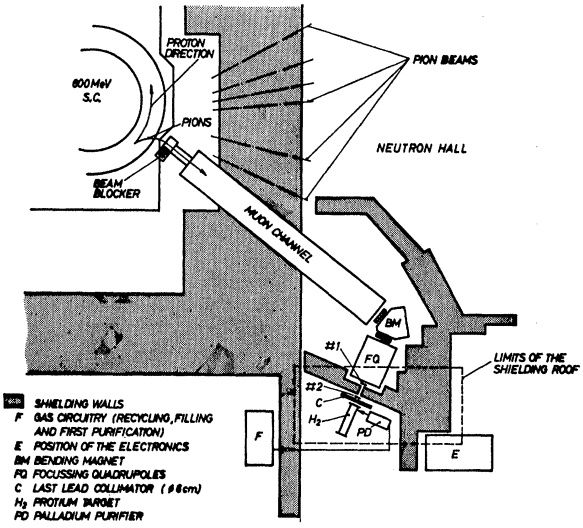

FIG. 5. Over-all view of the experimental layout on the synchrocyclotron floor, showing beam optics and shielding arrangements.

In order to compensate for the big delays introduced by the time fluctuations of the anticoincidence proportional counters, high impedance cables[32] were used throughout the whole electronics.

In the following, a *neutral trigger* indicates a pulse coming from the trigger coincidence when (i) the electronics was working in the neutral-selection way, (ii) a pulse coming from any of the A_i counters closed the gate to the GD discriminator, and (iii) the trigger signal started the sweeps of two double-beam oscilloscopes[33] and the recording, in digitized form, of the useful quantities.

An *electron trigger* was obtained when (i) the electronics was working in the electron selection way, (ii) the pulses from the A_i counter corresponding to the selected telescope could not switch off the gate to GD, (iii) the γ_i proportional counter facing the (A_i, N_i) telescope was disconnected from its preamplifier, and (iv) the trigger signal did not drive the two oscilloscopes, but still started the digitized recording of the useful quantities.

It is clear from the description that the TN_i pulses, essential for the neutron–γ-ray discrimination, were not used in the trigger logic. In both the neutral and the electron selections, the time interval between the mustop signal and the pulse coming from the N_i counters was measured by a time-to-pulse-height converter

[32] 950-Ω cables supplied by Suhner, Herisau, Switzerland, and 2900-Ω cables supplied by Hacketal, Hanover, Germany.

[33] A 555 and a 551 Tektronix oscilloscope.

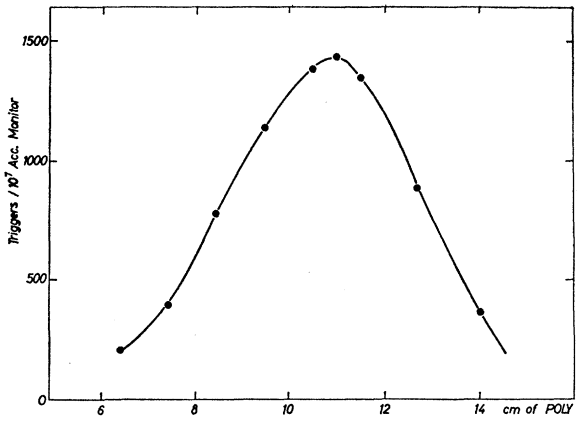

FIG. 6. Plot of the number of electrons counted by the electron telescopes as a function of the thickness of the poly absorber.

(TPHC), which was frequently checked by means of calibrated delay cables. The TPHC output pulse was sent to an encoder. Special care was taken to ensure that the origin of the time intervals registered by the encoder should be the same (within one channel) in the neutral trigger and electron trigger conditions. Checks were made on the linearity of the TPHC, also by studying the flat distribution due to the uncorrelated pulses of two different radioactive sources sent separately to the start and stop inputs of the circuit.

E. Muon Beam

The experiment has been performed at the muon channel of the CERN 600-MeV synchrocyclotron,[34] which was operated with a duty cycle of about 30%. The 130-MeV/c negative muon beam was focused towards a zone of the experimental hall where previous measurements had shown that the local background was sufficiently low to allow the capture experiment. The muons were collimated by a lead collimator having a diameter of 6 cm in its last section (see Fig. 5).

A poly absorber slowed down the muons before they entered the target. A beryllium moderator, 1 cm thick, was used as the last absorber so as to minimize losses due to multiple scattering; the beryllium moderator was placed inside the gaseous target at about 7 cm before counter α, which actually defined the beam entering the useful region of the target. The thickness of the carbon moderator was optimized by looking at the number of decay electrons detected by the electron telescopes in the electron trigger condition. A typical range curve obtained in this way is shown in Fig. 6.

To reduce the number of useless master pulses, the threshold of the discriminator of counter α was set so that it accepted only incoming muons with very high specific ionization, which were then likely to stop in the hydrogen. Such a level was chosen while looking at the decay electron rate. The main counting rates of significance with regard to the beam conditions are listed in Table IV.

[34] A. Citron, M. Morpurgo, and H. Øveros, CERN Report No. CERN 63-35, 1963 (unpublished). The pion contamination of the beam was less than 0.5%.

TABLE IV. Counting rates of the main circuits connected to the beam in the present muon-capture experiment.

Total beam in the (1,2) telescope (particles/sec)[a]	Total beam at the entrance of the useful region V (1,2,α) (particles/sec)	Total counts (1,2,$\sim\sum A_i,\alpha,\bar{\beta},\bar{\gamma}$) (particles/sec)
10 000	1 500	20

[a] The synchrocyclotron was operating with a duty cycle of 30%.

Note that the useful volume V' of the target contributing to the counts of the (A_i,N_i) electron telescope was slightly bigger than the volume V because of the additional volume of the γ_i counter. To estimate this small correction, a special run was done in which the electron yield was measured while all the γ_i counters were switched off (total electron trigger).

3. DATA RECORDING AND MEASUREMENTS

The output pulses of the main coincidence and anticoincidence circuits were stored by a set of scalers, the contents of which were recorded every 10^7 accepted monitors.

When the apparatus was set to work in the neutral trigger condition, the following data were then recorded.

(i) A picture of the two double-beam oscilloscopes was taken for each trigger. The first two sweeps, each 55 μsec long, displayed the outputs of the β and γ proportional counters. In this way the analysis of the pictures made it possible to increase their anticoincidence efficiency by recognizing those cases in which the electronic anticoincidences had failed because of the large time jitter of the proportional counters.
The other two tracks (21 and 11 μsec long, respectively) received the monitor pulse, a fast-neutron pulse, and, as it came out from the integrator, the AN_i pulse amplitude of the neutron counter responsible for the trigger. A system of four lamps was displayed on the pictures, indicating to which neutron counter the trigger was due.

(ii) For each trigger, the time interval measured by the TPHC and AN_i and TN_i amplitudes were recorded on paper tape in digitized form, and a proper system of ordering the events was foreseen so as to associate the digitized output with the corresponding picture.

When the apparatus was working in the electron trigger condition for one of the electron telescopes, the only information recorded was the time interval measured by the TPHC circuit (also in digitized form).

The measurements were performed either with pure protium or with protium contaminated by 10^{-3} parts

of pure xenon.[35] The measurements can be divided into the following four runs according to the gases filling the target and to the conditions of the electronics.

Run 1: Neutral Trigger, Pure Protium

Most of our running time was spent in these conditions, since the N neutrons attributable to reaction (1) were selected from the events obtained in these runs. In a special run, where one of the γ_i counters was switched off, neutrons arriving at earlier times were selected. In this way it was possible to collect events due to neutrons coming from nuclear captures of negative muons by iron nuclei (iron run).

Run 2: Electron Trigger, Pure Protium

Measurements in these conditions were frequently taken alternately with those described for run 1; these data supplied us (per accepted monitor) the number of μp muonic atoms which decayed, sending the electron into the chosen electron telescope. Moreover, in these conditions and during a special run, the counting rates of the electron telescopes were recorded as function of the thickness of additional different thin absorbers (iron, plastic, and glass) placed between the A_i counters and the hydrogen target. Counts were also taken for different values of the biases applied to the neutron counters, in order to deduce the loss in efficiency due to our working bias conditions (LT=0.4 MeV, electron energies).

Run 3: Neutral Trigger, Xenon-Protium

The transfer rate of a negative muon from a μp system to a xenon atom was in this case equal to $\lambda_{Xe} \simeq 10^7$ sec^{-1}.[36] In a very short time, therefore, all the negative muons stopped in hydrogen and forming μp muonic atoms were transferred to the xenon atoms, where they were quickly captured.[37] These measurements were therefore particularly suitable for obtaining a direct knowledge of the accidental neutrons, especially of their energy spectrum and time distribution.

Run 4: Electron Trigger, Xenon-Protium

These measurements were supplied mainly to check that all the electrons counted in run 2 were actually coming from muons bound in μp mesoatoms. In fact, after having added the xenon, the electrons showing a time distribution with a 2.2-μsec lifetime disappeared (see Fig. 7).

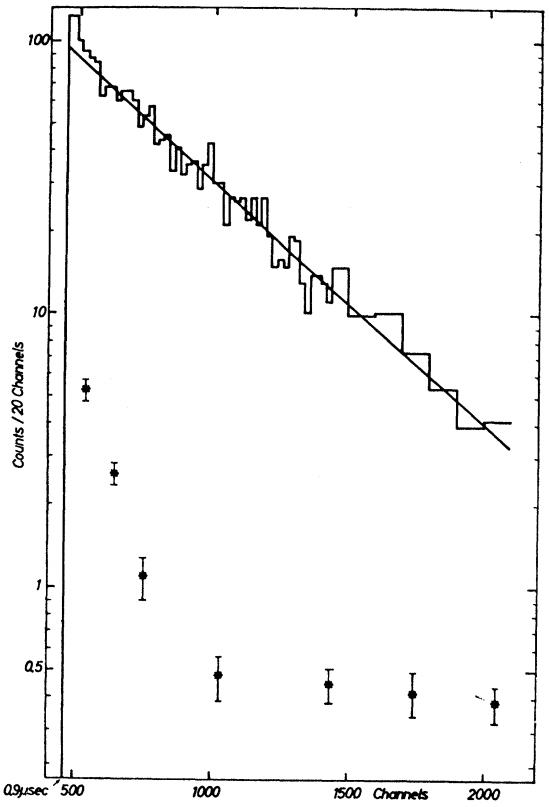

FIG. 7. Time distribution of the detected decay electrons coming from muons stopping in gaseous protium at 8 atm, and corresponding to 2×10^7 accepted monitors. The straight line represents a lifetime of 2.2 μsec. The separate points under the histogram represent the measured time distribution of the electrons detected after contaminating the protium with 10^{-3} parts of xenon, and for the same number of accepted monitors. The TPHC figure was 4.95 nsec/channel.

4. ANALYSIS

A. Analysis of Neutral Events

The pictures taken in run 1 were repeatedly scanned to select those in which no β or γ anticoincidence pulse was present in a fiducial time interval of the first two tracks. Pictures showing more than one neutron counter recognition lamp were rejected. Furthermore, during the scanning a check was made from time to time on performances of the encoders and on the TPHC circuit; this was done by measuring, on the third and fourth tracks of the pictures, the time intervals and the amplitudes of the AN_i pulses, and by comparing the results of these measurements with the digitized values printed on paper tape. Afterwards, a further selection was made by choosing only those events for which the AN_i amplitudes were contained between the limits of 0.72 and 3.7 MeV (electron energies).

The lower threshold was fixed at this value for the following reasons: (i) the contribution to the counting rate due to the accidental neutrons and γ rays, and to neutrons coming from the direct capture of negative

[35] The performance of the proportional counters was not appreciably affected by a small contamination of pure xenon in the protium.

[36] A. Alberigi Quaranta, A. Bertin, G. Matone, F. Palmonari, A. Placci, P. Dalpiaz, G. Torelli, and E. Zavattini, Nuovo Cimento **47B**, 92 (1967).

[37] J. C. Sens, Phys. Rev. **113**, 679 (1959).

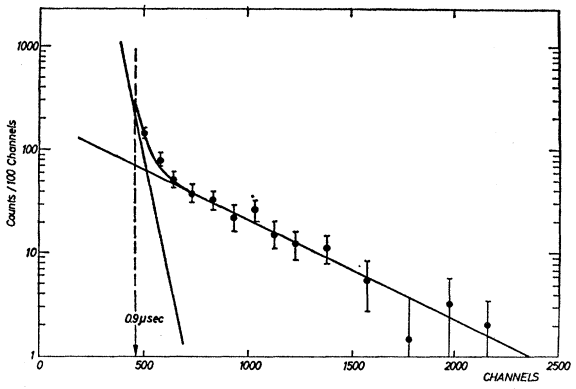

FIG. 8. Experimental time distribution of the neutron events after subtraction of the accidentals. The two straight lines correspond to the two components with 0.2 μsec (iron events) and 2.2 μsec (hydrogen events) lifetime. The TPHC figure was 4.95 nsec/channel. The arrow shows the time cut used in the analysis.

muons stopping in the stainless-steel wires of the proportional counters, started to be important below this level; (ii) the neutron-γ pulse-shape discrimination efficiency of our apparatus became poor below 0.7 MeV.

It should be mentioned that 0.72 MeV was close to the energies of the Compton peaks of the calibration sources used (^{22}Na, ^{60}Co); in this way it was possible to check directly the energy corresponding to our electronic bias.

The next step was that of selecting neutrons from γ rays in the remaining events, accepting only those for which the AN_i and TN_i amplitudes located a point in the neutron band of the (AN_i,TN_i) plot.

The events surviving all these selections were due to the following sources: (i) neutrons emitted in reaction (1), (ii) neutrons coming from nuclear capture of muons stopped directly in the wires of the proportional counters, and (iii) accidental neutrons.

To resolve these three components, the experimental time distribution of the selected events was fitted, using an expression formed by the sum of a constant term plus two negative exponentials with time constants of 2.2 μsec ($=1/\lambda_0$) and 0.2 μsec.[22] A small correction was also included in the fitting expression to take into account the possibility that the GD could be closed by a second monitor before the good event was detected.

The level of the accidental neutrons was also determined separately by analyzing the events obtained in run 3.

From these analyses it was found that the number N of detected neutrons due to nuclear capture of negative muons by free protons, and coming after 0.9 μsec from the stopping time of a negative muon in hydrogen, was

$$N=315\pm23. \tag{7}$$

The accidentals were found to be 29.1 events/μsec, and the total number of neutrons coming from nuclear captures in iron and detected after the same time was 95.

Figure 8 shows the experimental time distribution of the events after the accidentals were subtracted out. The quoted error on N includes also the error due to the uncertainty within which the level of the accidental counts was known. The total number of accepted monitors corresponding to these events was

$$M^*_{\text{tot}}=4521.75\times10^6. \tag{8}$$

The energy distribution of the pulses due to accidental neutrons collected in run 3 is shown in Fig. 9(a). A similar analysis was done for the events collected during the special iron run (see Sec. 3); the energy distribution of pulses due to neutrons coming from captures of muons by iron nuclei is given in Fig. 9(b).

The experimental energy spectrum of the pulses due to the 315 events recognized as neutrons coming from reaction (1) is shown in Fig. 10; it has been obtained by subtracting (properly normalized) the accidental and iron energy spectra from the spectrum of the total events.

It is worth pointing out that the events falling in the γ band of the (AN_i,TN_i) plot (selected in amplitude and time as the finally accepted N neutrons) and showing a 2.2-μsec lifetime, totalled about 350. Therefore, the neutron-γ discrimination technique turned out to be essential; on the other hand, its selection efficiency of neutrons versus γ rays was quite adequate.

B. Analysis of Electron Events

The time analysis of the events collected during run 2 showed that these events contained 2% of accidentals, and that towards the earliest times a small contribution of electrons coming from muons stopping directly in iron was present (see, for instance, Fig. 7).

The number n_e of electrons coming from μp systems formed within the volume V and counted by our elec-

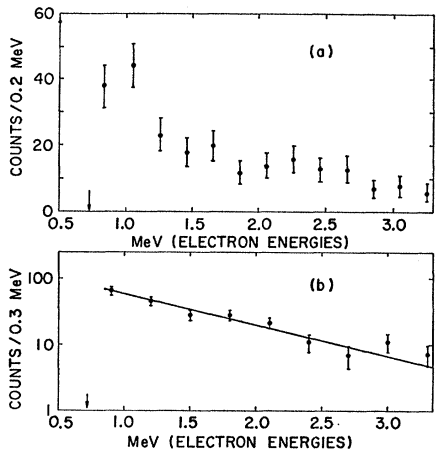

FIG. 9. (a) Energy distribution of the pulses due to accidental neutrons. (b) Energy distribution of the pulses due to neutrons coming from capture of muons in iron. The straight line represents an exponential energy distribution $N_0\exp(-E/0.9)$ obtained by a best-fit analysis. The arrows indicate the lower-energy cut used in the analysis.

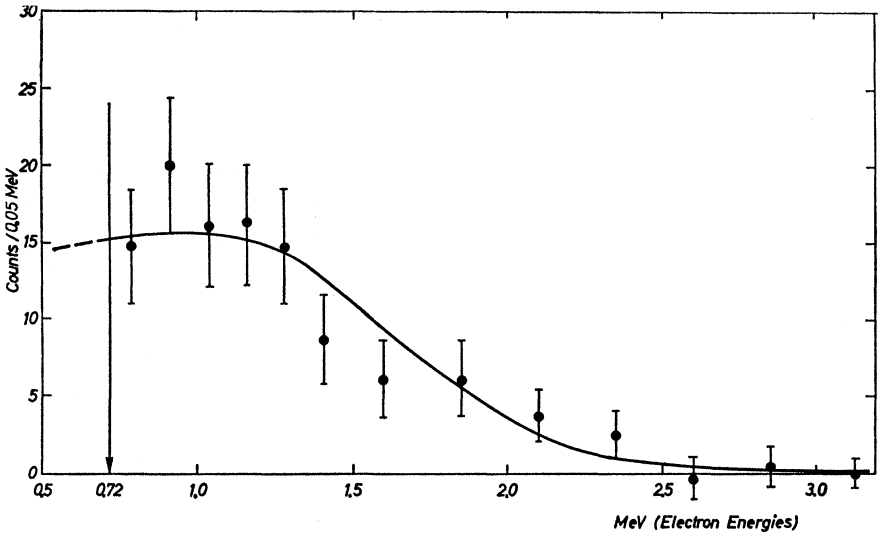

FIG. 10. Experimental energy spectrum of the pulses due to the 315 neutrons coming from reaction (1). The low-energy cut effected in the analysis is shown by the arrow. The solid line represents the calculated expected amplitude spectrum (normalized to the number of events) assuming for the pulse-height response curve of the NE-213 liquid scintillator, curve *c* of Fig. 11. The spatial distribution of the muons's stopping points (within the accepted region V of the hydrogen gas target) has been calculated as specified in the text.

tron telescope after 0.9 μsec following their formation (within a 10-μsec interval) was

$$n_e = 1120 \text{ per } 10^7 M^*. \tag{9}$$

This number was obtained after performing a small geometrical correction (see next paragraph); the statistical error on n_e was smaller than 1%.

The over-all efficiency E_e of our electron telescopes appearing in Eq. (6) can be written as

$$E_e = \Omega_e W, \tag{10}$$

where Ω_e is the solid angle for the electron detection, and W is a factor which takes account of losses due to both the electronic bias and the materials present between the N_i detectors and the hydrogen. From the special measurements performed in run 2 we obtained

$$W = (74 \pm 2)\%. \tag{11}$$

A simplified calculation, also taking into account the fact that the electrons detected by our telescopes crossed the various materials present along their path with an average angle of incidence of about 45°, fully justified the value given in Eq. (11).

C. Computation of the Efficiencies

In order to deduce the Λ_{expt} value from Eq. (6), both the over-all efficiency E of the apparatus to count neutrons and the solid angle Ω_e of the electron telescopes were still needed. These quantities were evaluated taking account of the specifical geometry of the apparatus (see Figs. 1 and 2); we now give a brief outline of how these calculations were done.[38]

As a first step, the spatial distribution of the muons stopping in the volume V was determined by a Monte Carlo calculation, which followed the muon from the entrance of the carbon moderator until either it left V or stopped in it. The energy spread and the spatial distribution of the beam at the entrance to the carbon absorber were known from measurements. In the calculation, one considered also the multiple scattering effects introduced by the carbon and beryllium absorbers, and the limitations introduced by the different cylindrical collimators. Only those muons passing through the first grid of the α proportional counter were finally accepted. The beam was assumed to have a cylindrical symmetry around the axis of the target; it is clear that small deviations from such configuration could not affect the final results because of the symmetry of the neutron and electron detectors around the axis of the target.

The results of this first calculation were then used as input data to deduce the efficiency E, the total solid angle Ω_e, and some small geometrical corrections to the experimental yield of electrons. Such corrections were due to the difference between the V' volume effective in the electron trigger condition and the useful volume V to be considered in the neutral trigger condition; this difference existed because in the former case one of the γ_i counters was switched off, and also because there were edge effects in the remaining γ_k counters. The calculation pertaining to these corrections showed that the experimental yield had to be corrected for about 5%. This result was checked by comparing it with the measured ratio between the yield of the 2.2-μsec time component obtained in the electron trigger condition, and the corresponding yield obtained in the total electron trigger condition (see end of Sec. 2).

The total solid angle of the electron telescopes, taking into account the spatial distribution of the stopping muons, turned out to be

$$\Omega_e = 12.0\%. \tag{12}$$

[38] All the calculations were performed using the 6600 CERN computer, the 7094 Bologna computer (Centro di Calcolo del CNEN), and the 7090 CNUCE Pisa computer.

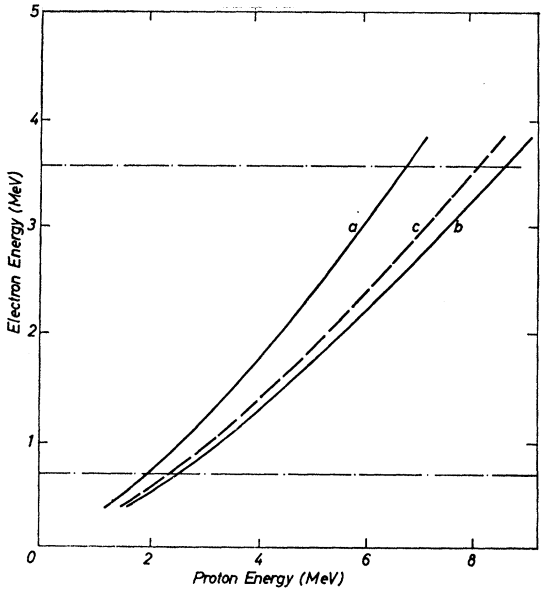

FIG. 11. Pulse-height response of the NE-213 liquid scintillator to protons: (a) Rothberg result; (b) Batchelor result; (c) result obtained in the present experiment. The horizontal lines indicate the interval of energies corresponding to the accepted AN_i amplitudes.

A Monte Carlo calculation was done to evaluate the over-all efficiency E, following the neutron from its production point until it had either slowed down to energies lower than 0.05 MeV, or it had left the apparatus.[39] The geometrical figures considered in the calculation included the complete target, the anticoincidence plastic scintillator counters A_i, the neutron detectors's volumes and their walls, the lead shielding surrounding the detectors, and the paraffin.

To complete the calculation of E it was necessary to know, besides the energy resolution and biases of the neutron counters, their response as a whole detecting system (liquid scintillator, photomultipliers, and related electronics) to protons of energies between 0.05 and 5.2 MeV, i.e., to know the ratio of the energies of protons and electrons which produced the same AN_i amplitudes. This response was measured[4,40] by different authors; we could not, however, assume *a priori* any of the results obtained, since they certainly depend on the purity of the liquid scintillator cells used, and on the particular circuitry employed to obtain the AN_i amplitudes [in particular, in our case the response can depend on the $(t_0$–$t_3)$ gating times; see Sec. 2)].

Different amplitude spectra for the neutron counters were therefore produced by the Monte Carlo calculation, using different pulse-height response curves of the NE-213 liquid and electrons. These curves were obtained by linear interpolation between the curve given by Rothberg *et al.*[4] and the one given by Batchelor *et al.*[40] A χ^2 analysis has shown that the spectrum, among the calculated ones, that best fits our experimental spectrum of Fig. 10 is the one obtained assuming the pulse-height response curve c shown in Fig. 11; this response curve turned out to be similar to the one found by Batchelor.

The value finally obtained for E was[41]

$$E=(3.90\pm0.15)\%. \tag{13}$$

The quoted error was estimated by varying the main parameters in the Monte Carlo calculation for E, and looking at their influence on the efficiency itself.

5. RESULTS AND CONCLUSIONS

The main results of the measurements and of the calculations described in the previous sections are $N=315\pm23$, $E=(3.90\pm0.15)\%$, $N_e=n_e(M^*_{\rm tot}/10^7)=(5.07\pm0.05)\times10^5$, $E_e=\Omega_e W(8.88\pm0.27)\%$, and $l=1.01$.

From these values, and using Eq. (6), one gets

$$\Lambda_{\rm expt}=651\pm57\ \text{sec}^{-1}, \tag{14}$$

where the error is calculated by adding quadratically the errors given in the above list. Referring to this value, we can draw the following conclusions:

(a) Our experimental result [Eq. (14)] agrees within the error with the value

$$\Lambda_{s,\rm theor}=626\pm26\ \text{sec}^{-1} \tag{15}$$

obtained by Kabir,[13] which was derived assuming

$$f=\frac{g_p}{g_V}=-\frac{4}{g_V}\frac{G_{NN\pi}}{m_\pi{}^2-q^2}\times\left(\frac{\pi}{m_\pi{}^2\tau_\pi}\right)^{1/2}\left(1-\frac{m_\mu{}^2}{m_\pi{}^2}\right)^{-1}=-9.1, \tag{16}$$

where g_p is the induced pseudoscalar couping constant,[42] g_V is the vector coupling constant, $G_{NN\pi}$ is the pion-nucleon coupling constant, m_π and m_μ are the masses of the pion and of the muon, respectively, and τ_π is the pion lifetime;

$$r=g_A/g_V=-1.18\pm0.02, \tag{17}$$

where g_A is the axial-vector coupling constant,[43] and

$$g_V=(1.0034\pm0.0016)\times10^{-5}/M^2, \tag{18}$$

where M is the proton mass.[44]

[39] Proper neutron elastic and inelastic scattering cross sections were used for each element considered in the calculations taken from *Neutron Cross Sections* (Brookhaven National Laboratory, Associated Universities, Inc., New York, 1966).

[40] R. Batchelor, V. B. Gilboy, J. B. Parker, and J. H. Towel, Nucl. Instr. Methods 13, 70 (1961).

[41] Note that the contribution to E of that part of the lead shielding near the neutron counters (within 15 cm) is about 10% of E, due to the neutrons diffused by the lead itself into the N_i counters.

[42] L. Wolfenstein, Nuovo Cimento 8, 882 (1958).

[43] C. S. Wu, cited by S. L. Adler, Phys. Rev. Letters 14, 1051 (1965).

[44] J. Freeman, J. Montague, G. Murray, R. White, and W. Burcham, Phys. Letters 8, 115 (1964).

TABLE V. The different values of the ratio $T=(\Lambda_{t,\text{theor}}/\Lambda_{s,\text{theor}})$ which one determines by combining the Λ_{expt} nuclear capture rate measured in the present experiment, with the $\Lambda_{M,\text{expt}}$ rates obtained in the preceding experiments of nuclear capture of muons in liquid hydrogen.[a]

Reference expt.	T
Chicago	-0.37 ± 0.6
CERN-Bologna	-0.23 ± 0.4
Columbia	-0.18 ± 0.36

[a] See Table I.

(b) Within the experimental error, there is consistency between the experimental value Λ_{expt} [Eq. (14)] and the $\Lambda_{M,\text{expt}}$ values reported in Table I. In fact, $\Lambda_{M,\text{theor}}$ is given by[10]

$$\Lambda_{M,\text{theor}}=2\gamma_0(\tfrac{3}{4}\Lambda_{s,\text{theor}}+\tfrac{1}{4}\Lambda_{t,\text{theor}}), \quad (19)$$

where $2\gamma_0=1.01\pm0.01$,[13] and $\Lambda_{s,\text{theor}}$ and $\Lambda_{t,\text{theor}}$ are given in Table I; combining then the present experimental result with the values obtained in the liquid-hydrogen experiments (see Table I), one can determine an interval of values within which must be included the ratio

$$T=\Lambda_{t,\text{theor}}/\Lambda_{s,\text{theor}}, \quad (20)$$

which by definition is a positive quantity. Such values

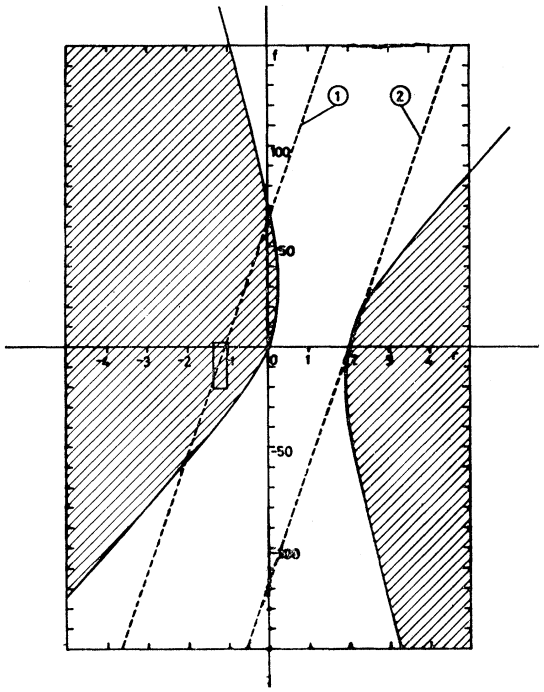

FIG. 12. The shaded area represents the region allowed for all possible pairs of $f=g_p/g_V$ and $r=g_A/g_V$, and for any choice of g_V by the limitation (21) $0\leq\Lambda_{t,\text{theor}}/\Lambda_{s,\text{theor}}\leq0.4$ obtained by combining the experimental results of the liquid-hydrogen experiments and of the present one. The small rectangle indicates the region covered by Fig. 13. The two dashed straight lines 1 and 2 represent the pairs of r and f values allowed by the present experimental result $\Lambda_{\text{expt}}=651$ sec^{-1} if g_V is given by Eq. (18). It is clear that the values represented by line 2 are excluded by limitation (21).

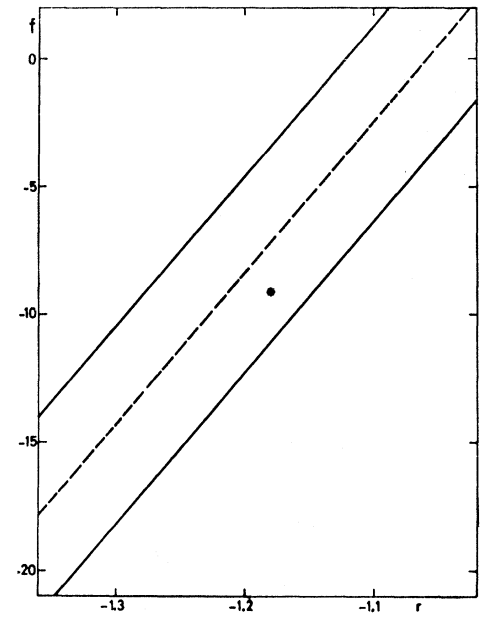

FIG. 13 Variations of $f=g_p/g_V$ and $r=g_A/g_V$ allowed by the observed value $\Lambda_{\text{expt}}=651\pm57$ sec^{-1} assuming g_V as given by Eq. (18). The theoretical value obtained by Kabir (Ref. 13) is shown by the asterisk.

are listed in Table V. Figure 12 shows, independently from the value of g_V, all the possible pairs of f and r values (shaded area) which are consistent with the limitation

$$0\leq T\leq0.4, \quad (21)$$

the upper limit being fixed by the experiments.

Recently, it has again been suggested[45] that the ratio r to be used in predicting the rate of the capture process (1) should be taken equal to $+1.18$. Figure 12 shows that the hydrogen experiments exclude such a value for r and for any choice of f and g_V. A similar conclusion was already reached by Culligan *et al.*[46] looking at the nuclear capture of negative muons by ^{19}F. A recent analysis of muon-capture experiments in various nuclei[47] yielded the same conclusion.

It is worthwhile mentioning that $\Lambda_{M,\text{expt}}$ can be compared to the theoretically predicted value [Eq. (19)] only if initially the $p\mu p$ muonic molecules are all formed in an ortho state,[48] and if the ortho- to para-state transition rate Λ_{op} for the muonic molecules is negligible compared to the decay rate λ_0 of the free muon. Theoretical investigations have set an extremely small upper limit[7,9] for Λ_{op}, whereas the experimental results

[45] N. P. Chang, Phys. Rev. Letters **16**, 337 (1966).

[46] G. Culligan, J. F. Lathrop, V. L. Telegdi, R. Winston, and R. A. Lundy, Phys. Rev. Letters **7**, 458 (1961).

[47] P. Pascual and R. Pascula, Phys. Rev. Letters **16**, 1057 (1966).

[48] The $p\mu p$ muonic molecules can be either in an ortho state ($J=1$, $S=0$) or in a para state ($J=0$, $S=1$). (See Refs. 7 and 9). When all the $p\mu p$ molecules are in the para state, Eq. (17) should be written $\Lambda_{M,\text{theor}}=2\gamma_p(\frac{1}{4}\Lambda_{s,\text{theor}}+\frac{3}{4}\Lambda_{t,\text{theor}})$, where γ_p is about 10% larger than γ_0 (Ref. 11).

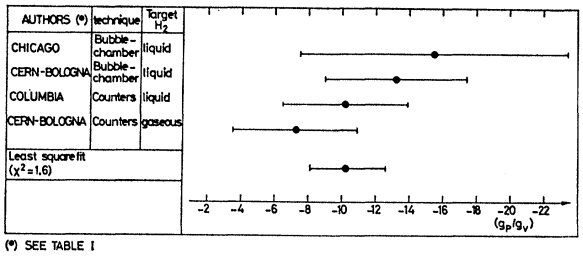

FIG. 14. Summary of the results for the ratio $f=g_p/g_V$ obtained from the muon-capture experiments listed in Table I.

to date give[2,4]

$$\Lambda_{op}\leq 5\times 10^4 \text{ sec}^{-1}. \quad (22)$$

A value of Λ_{op} equal to the upper limit (22) (assuming that all the $p\mu p$ muonic molecules are initially formed in an ortho state) would lower the $\Lambda_{M,\text{theor}}$ value quoted in Table I by about 9%.

(c) From the experimental value Λ_{expt} [Eq. (14)], assuming for r and g_V the values given in Eqs. (17) and (18), one deduces for g_p the following value:

$$g_p=(-7.3\pm 3.7)g_V, \quad (23)$$

which is in good agreement with the value given in Eq. (16). A second solution ($g_p=-190\ g_V$) is ruled out by the limitation (21). The dependence of g_p on r is given in Fig. 13.

By analyzing in the same way the other results listed in Table I, which correspond to a different total spin state of the initial muon-proton system one obtains for g_p the values shown in Fig. 14.

From the fact that g_V and g_A have been assumed equal to the corresponding values deduced from experiments on β-decay processes,[43,44] one infers that the agreement between the different experimental results of Fig. 14 and the calculated value $g_p=-9.1\ g_V$ can be considered, within the confidence which one gives to the one-pion-exchange approximate formula (16) and within the experimental errors, as direct evidence of the μ-e universality in strangeness-conserving weak-capture processes.

Notwithstanding the reservations on $\Lambda_{M,\text{theor}}$ expressed above, we have combined the values given in Fig. 14 together by a least-squares fit procedure, obtaining for g_p

$$\bar{g}_p=(-10.5\pm 2.2)g_V. \quad (24)$$

Regarding the experimental determination of g_p from the capture of negative muons by other elements: Looking at those channels particularly sensitive to the value of g_p, it appears that (i) the experimental results[49] obtained by studying the muon capture in ^{16}O are consistent with a value for g_p close to the value of Eq. (16); and (ii) Conversi *et al.*,[50] studying the radiative capture of negative muons in ^{30}Ca, obtained

$$g_p=(13.3\pm 2.7)g_A, \quad (25)$$

from which, using Eq. (17), one gets

$$g_p=(-15.1\pm 3.2)g_V,$$

in fair agreement with the value given by Eq. (24).

ACKNOWLEDGMENTS

The authors would like to thank O. Polgrossi, R. Schillsott, G. Sicher, and B. Smith for their skillful technical assistance, and Mrs. R. Vuaillet for her helpful cooperation in scanning the pictures. They are also particularly indebted to Professor P. Bassi, Professor P. Preiswerk, and Professor G. Puppi for their encouragement and support, and to Dr. J. Bell for helpful discussions.

[49] R. C. Cohen, S. Devons and A. D. Kanaris, Phys. Rev. Letters **11**, 134 (1963); Nucl. Phys. **57**, 255 (1964), A. Astbury, L. B. Auerbach, D. Cutts, R. J. Esterling, D. A. Jenkins, N. H. Lipman, and R. E. Shafer, Bull. Am. Phys. Soc. **9**, 81 (1964); Nuovo Cimento **33**, 1020 (1964).

[50] M. Conversi, R. Diebold, and L. Di Lella, Phys. Rev. **136**, B1077 (1964).